Monitoring the Role of Oxalate in Manganese Peroxidase

Lucia Banci,[‡] Ivano Bertini,*[,‡] Lorenzo Dal Pozzo,[‡] Rebecca Del Conte,[‡] and Ming Tien[§]

Department of Chemistry, University of Florence, Via Gino Capponi, 7, I-50121 Florence, Italy, and Department of Biochemistry and Molecular Biology, Pennsylvania State University, University Park, Pennsylvania 16802

Received November 25, 1997; Revised Manuscript Received April 14, 1998

ABSTRACT: The water proton relaxation rate measurements between 0.01 and 50 MHz on water solutions containing the cyanide adduct of the manganese-depleted manganese peroxidase (MnP−CN^-) and increasing amounts of Mn^{2+} have been determined. The proton relaxivity curves have shown evidence of the formation of the protein/Mn^{2+} complex and have been analyzed in order to obtain spin Hamiltonian parameters and correlation times. Oxalate is shown not to alter the above profiles. This suggests that no protein−Mn^{2+}−oxalate ternary complex is formed and that oxalate does not remove Mn^{2+} from the protein. On the basis of high-resolution ^{1}H NMR experiments, we propose that Ce^{3+} and Gd^{3+} bind at the manganese site, and, on the basis of the charge, we propose that they may mimic Mn^{3+}. The water proton relaxation rates of water solutions containing manganese-depleted MnP−CN^- and increasing amounts of Gd^{3+} have been measured and analyzed. Oxalate is shown to remove the trivalent metal ions. This suggests that trivalent metal ions bind oxalate and diffuse away from the protein presumably as oxalate complexes. Implications for the enzymatic mechanism are discussed.

Manganese peroxidases (MnPs) are produced by filamentous fungi and catalyze the oxidative depolymerization of the aromatic polymer lignin (*1*). MnP was first discovered in the fungus *Phanerochaete chrysosporium* (*2*, *3*), and the enzyme from this source has provided most if not all of the structural and kinetic information (*4*). MnP is unique in catalyzing the oxidation of divalent manganese to trivalent manganese (*5*). The structure of the heme region of MnP is typical of peroxidases with a five-coordinated iron ion coordinated to the "proximal" histidine (*6*). The "distal" side of the heme contains invariant histidine and arginine residues (*7*). These residues are involved in reactions with H_2O_2, which is required in the catalytic cycle (*8*−*11*). The X-ray structure has shown that the active cavity and most of the elements of secondary structure are very close to that of lignin peroxidase (LiP) (*6*), another isoenzyme produced by the same organisms and which does not need manganese in its catalytic cycle.

The catalytic cycle of MnP is similar to that of other heme peroxidases. The catalytic cycle involves initial two-electron oxidation of the heme by H_2O_2 to form compound I. Compound I contains the iron (IV)═O moiety and a cation radical on the porphyrin ring (*12*, *13*). Compound I then returns to ferric enzyme by two one-electron oxidation steps where two substrate molecules are oxidized by single electrons. The one-electron oxidized intermediate state of the enzyme is referred to as compound II which is the iron (IV)═O species (*14*).

The low-temperature EPR spectra of native MnP and LiP confirm an essentially identical high-spin ($S = {}^5/_2$) ferric coordination (*15*). Furthermore, the EPR spectrum appears to be axial, corresponding to a tetragonally symmetric heme environment, while the EPR spectra of other peroxidases as cytochrome *c* peroxidase (C*c*P) and horseradish peroxidase (HRP) show a large rhombic component (*15*, *16*). Resonance Raman results indicate that MnP and LiP have a more axial heme symmetry as compared with the other peroxidases (*15*, *17*) consistent with the EPR data. The EPR spectra of the cyanide adducts of peroxidases are typical of a low-spin heme iron (*16*). The NMR spectra of the unligated form of MnP and of the cyanide derivative are very similar to that of LiP (*18*−*20*) and are close, even if at a less extent, to those of C*c*P (*21*−*23*), HRP (*24*), and *Coprinus cinereus* peroxidase (CIP) (*25*).

The preferred substrate of MnP is divalent manganese. The binding site for Mn^{2+} is well-defined being identified by X-ray crystallography (*6*) which confirmed early NMR (*26*) and site-directed mutagenesis (*17, 27*) studies. NMR and structural analysis (*28*) reveal that small aromatic molecules can enter the active-site cavity of HRP between Phe 179 and the heme edge bearing 8-CH_3 (*26*, *29*, *30*, Andy Smith, personal communication). In contrast, only mutants of CcP can accommodate molecules such as styrene (*31*), while for LiP the binding site of aromatic substrates has yet to be identified. In MnP it has been demonstrated that only Mn^{2+} is capable of reducing compound II to the native enzyme (*32*). NMR data have shown that the affinity constant of Mn^{2+} to MnP is larger than 10^4 M^{-1} (*26*), consistent with the apparent dissociation constant (K_d) of 9.6 μM from kinetic measurements (*33*). The Mn^{2+} ion is coordinated by the carboxylate group of propionate 6, by the carboxylate of Glu 39, Glu 35, and Asp 179, and by two water molecules (*6*). Therefore, it seems likely that the electron flows through the Mn-ligated propionate 6 to the heme iron.

* To whom correspondence should be addressed. Phone: +39.55.2757549. Fax: +39.55.2757555. E-mail: bertini@risc1.lrm.fi.cnr.it.
[‡] University of Florence.
[§] Pennsylvania State University.

S0006-2960(97)02879-1 CCC: $15.00
Published on Web 06/02/1998

It has been shown that oxalate stimulates Mn peroxidase activity, that this organic acid is produced extracellularly by ligninolytic culture of *P. chrysosporium*, that the stimulation of Mn peroxidase activity occurs at micromolar concentrations of oxalate, and that the oxalate is able to support Mn peroxidase reaction in the presence of molecular oxygen even in the absence of H_2O_2 (*34, 35*).

In this report we investigate the nature of the manganese binding and the role of oxalate. Through measurements of water proton relaxation in the frequency transition range of 0.01−50 MHz (relaxometry measurements), we investigate whether oxalate replaces the water molecules and binds Mn^{2+}. The conclusion is that oxalate does not bind Mn^{2+} when coordinated to MnP, whereas it binds to tripositive ions such as lanthanides when bound to MnP. If the latter metal ions could be taken as probes for Mn^{3+}, then our experiments suggest that Mn^{2+} in MnP is oxidized by the enzyme to Mn^{3+}, which is then complexed by oxalate and taken away from the protein.

EXPERIMENTAL PROCEDURES

Production and Purification of Recombinant Mn peroxidase. Nonglycosylated recombinant manganese peroxidase was prepared using the recombinant MnP expression vector constructed by Whitwam et al. (1995) (*36*) with some minor modifications. The protein was expressed in *Escherichia coli* and refolded as previously reported (*36*). The recombinant protein was purified by three different steps. The first step involved anion-exchange chromatography on DEAE Bio-Gel A (1.5 × 20 cm) using a linear gradient of 0−150 mM $CaCl_2$ in 50 mM Tris pH 8. Column fractions with an absorbance greater than 1 at 407 nm were pooled and dialyzed against 50 mM Tris-Cl pH 8. Pooled fractions were further purified by a second DEAE Bio-Gel A column similar to the first. Column fractions with the highest ratio of 407 to 280 nm absorbance ($R_z = A_{407}/A_{280}$) were pooled and dialyzed against Milli-Q water. The third step consisted of a preparative flat bed isoelectric focusing. The activity of the protein was assayed using conditions previously described (*3, 37*). The purified MnP had an R_z value of about 5.5. The enzyme concentration was determined using the extinction coefficient at 407 nm of 127 mM^{-1} cm^{-1} (*3*).

The cyanide derivative of MnP was obtained by adding stoichiometric amounts of KCN.

Nuclear Magnetic Relaxation Dispersion (NMRD) Measurement. Such experiments consist of measuring the water proton relaxation rate at various magnetic fields. All ^1H NMRD profiles were measured with a Koenig-Brown field cycling relaxometer operating in the 0.01−50 MHz proton Larmor frequency range (*38*−*40*). The error in T_1 values is less than 2%. Sample volumes ranged from 0.35 to 0.45 mL and contained an initial MnP concentration of either 0.29 or 0.24 mM. Mn^{2+} titration was performed in 100 mM phosphate buffer at pH 6.5 by adding small volumes of a $MnSO_4$ stock solution (6.1 mM), while Gd^{3+} and Ce^{3+} titrations were performed in 25 mM Hepes at pH 5.8 by adding small volumes of a standard Gd^{3+} or Ce^{3+} solution (6.0 and 5.1 mM, respectively). Titrations with oxalate were performed by using a stock solution of oxalate (200 mM) at pH 5.8. The temperature was regulated by circulating perchloroethylene maintained at either 303 or 283 K.

Nuclear Magnetic Resonance (NMR). The ^1H NMR spectra of the cyanide adduct of MnP in 25 mM Hepes buffer, pH 5.8, were recorded with a Bruker DRX 500 spectrometer, operating at 11.7 T. All NMR experiments were collected with ^1H-presaturation sequence with a recycling time of 350 ms at 298 K. Proton chemical shifts are referenced to the H_2O signal at 4.81 ppm relative to tetra methyl silane (TMS). Gd^{3+} and Ce^{3+} titrations were performed by adding small volumes of a standard Gd^{3+} or Ce^{3+} solution (6.0 and 5.1 mM, respectively) and oxalate titrations were performed by adding increasing amounts of a stock solution of oxalate (200 mM) at pH 5.8. The MnP concentration in these titrations was 0.5 mM.

RESULTS

Relaxivity of MnPCN$^-$*−Mn*$^{2+}$. The interaction of Mn^{2+} with MnP had been previously studied through NMR measurements on the manganese-depleted protein (*26*) and on its cyanide derivative (*26*). Binding of Mn^{2+} gives rise to the broadening of the 3-CH_3 signal and to the disappearance of the 8-CH_3 signal. In the present study, the effect of Mn^{2+} addition on MnP−CN^- was investigated by ^1H NMRD at various Mn^{2+}/protein ratios.

We previously demonstrated that manganese binding to MnP is not affected by the coordination of cyanide (*26*). Consequently, we have decided to perform all the relaxivity experiments on the cyanide derivative of MnP which was better investigated through high-resolution NMR studies (*26*).

The results indicate that the enhancement on water proton relaxivity due to Mn^{2+} binding is linearly dependent on its concentration. From the dependence of the relaxation enhancement on the Mn^{2+} concentration, an affinity constant of about 8×10^4 M^{-1} can be estimated. This value is in complete agreement with the value obtained from kinetic and high-resolution NMR data (*33*). The NMRD enhancement profiles are obtained by subtracting the profiles of the Mn^{2+}-free protein solution from each protein−Mn_x ($x < 1$) profile. These values, normalized to 1 mM metal ion concentration, are reported in the ordinates of the relaxivity figures. The contribution to relaxivity of the water protons due to the $Mn(OH_2)_6^{2+}$ species appears as a slight inflection at low fields as due to contact dispersion (*39, 41*). The amount of Mn^{2+} not coordinated to the protein was estimated from the affinity constant (taken equal to 8×10^4 M^{-1}, as it results from the NMRD titration), and its contribution to relaxivity was subtracted.

The NMRD profiles of the MnPCN$^-$−Mn^{2+} system at two temperatures are shown in Figure 1. The profiles can be interpreted with the Solomon equation (*42*) which describes the nuclear relaxation rates, T_{1M}^{-1}, due to the dipolar coupling of one proton with the unpaired electrons, *S*,

$$T_{1M}^{-1} = \frac{2}{15}\left(\frac{\mu_0}{4\pi}\right)^2 \frac{\gamma_n^2 g^2 \mu_B^2 S(S+1)}{r^6} \times \left[\frac{7\tau_c}{1+\omega_S^2\tau_c^2} + \frac{3\tau_c}{1+\omega_I^2\tau_c^2}\right] \quad (1)$$

where ω_I and ω_S are the proton and electron Larmor frequencies, r is the proton−metal distance, and τ_c is the correlation time for the dipolar coupling, which is determined

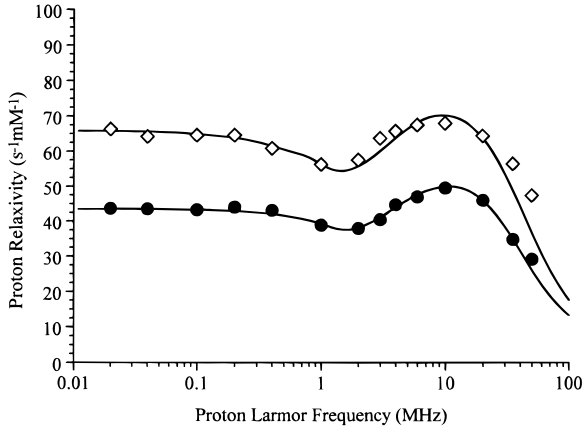

FIGURE 1: Proton relaxivity profiles of a water solution containing the $MnPCN^{-}-Mn_{0.8}^{2+}$ adduct, normalized at a 1 mM metal ion concentration, in 100 mM phosphate buffer, pH 6.5, at 303 (◇) and 283 (●) K. The lines represent the best fit curves with the parameters reported in Table 1.

by the shortest between the electron (τ_s), the rotational (τ_r), and the exchange (τ_m) correlation times. The other symbols have the usual meaning. In the present case, as it is generally true for metalloproteins, τ_s is the correlation time for the relaxation rates at low magnetic fields. The Bloembergen−Morgan equation, which describes the electron relaxation rates in solution as a function of magnetic field (*43*), is

$$\tau_s^{-1} = \frac{2\Delta^2(4S(S+1)-3)}{50}\left(\frac{\tau_V}{1+\omega_S^2\tau_V^2}+\frac{4\tau_V}{1+4\omega_S^2\tau_V^2}\right) \quad (2)$$

where Δ^2 is the average quadratic transient zero field splitting (ZFS) and τ_v is the correlation time for the coupling between the electron spin and the lattice. The quantity $(^1/_5)\Delta^2(4S(S+1)-3)\tau_V$, also called $\tau_{S_0}^{-1}$, is the low-field limit of the electron relaxation rates.

The NMRD profiles reported in Figure 1 are typical profiles for one or more water molecules interacting with a Mn^{2+} ion bound to a slowly rotating system. The profiles show an inflection around 1 MHz due to the ω_s dispersion of eq 1 (*39*), then an increase in relaxivity due to the increase of τ_s according to eq 2, and finally the decrease due to the ω_I dispersion of eq 1. The position of the bell-shaped curve defines the τ_v value. The presence of zero field splitting (ZFS) influences the actual values of relaxivity at low magnetic fields and the depth of the saddle (*44*). An increase in nuclear relaxation rates with increasing temperature is observed, which indicates that the paramagnetic effect on nuclear relaxation, T_{1p}^{-1}, depends on τ_m, according to the following equation (*39*):

$$T_{1p}^{-1} = f(T_{1M}+\tau_m)^{-1} \quad (3)$$

In other words, one or two water molecules exchange with a time comparable to T_{1M}.

Such profiles can be simulated or best fit with a program made available in our laboratory (*45*) that includes ZFS effects. The parameters which define the NMRD curves are many and some of them are covariant. Here, we want to show that the X-ray structure, with two water molecules bound to Mn^{2+}, is consistent with the present experimental data. The best fitting, reported in Figure 1, is obtained by assuming that (i) the rotational correlation time τ_r, at the two temperatures, is given by the Stokes−Einstein equation (*46*, *47*):

$$\tau_r = \frac{4\pi\eta a^3}{3kT} \quad (4)$$

where η is the viscosity of the solvent, a is the radius of the molecule, k is Boltzmann constant, and T is temperature; (ii) the zero field splitting parameter (D) is taken to be equal for the two temperatures; and (iii) there are two water molecules which have the same exchange correlation time τ_m.

Table 1: Best Fitting Parameters of the ^{1}H NMRD Profiles of the $MnPCN^{-}-Mn^{2+}$ Systems

temperature (K)	303	283
τ_r (s)	1.34×10^{-8}	2.35×10^{-8}
τ_V (s)	7.5×10^{-11}	7.9×10^{-11}
Δ (cm^{-1})	8.1×10^{-3}	1.1×10^{-2}
D^a (cm^{-1})	1.2×10^{-2}	1.2×10^{-2}
τ_m (s)	5.1×10^{-7}	7.9×10^{-7}
r (Å)	2.80	2.80

[a] D is the static ZFS parameter.

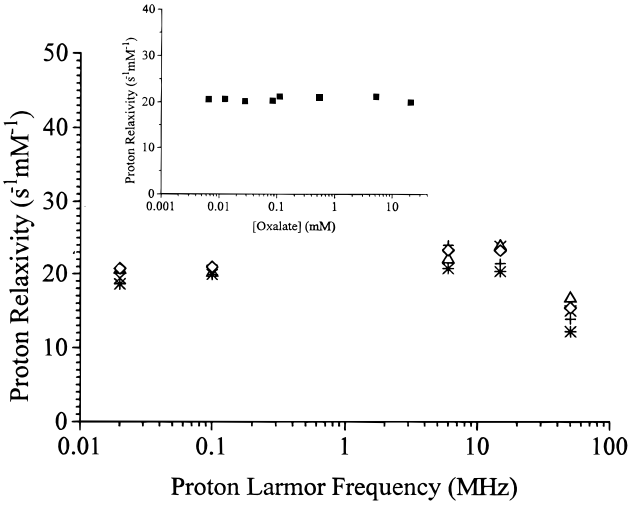

FIGURE 2: Proton relaxivity of a water solution containing the $MnPCN^{-}-Mn_{0.8}^{2+}$ adduct, normalized at a 1 mM protein concentration, in 100 mM phosphate buffer, pH 6.5, at 303 K at different concentrations of oxalate: (×) protein without oxalate and (△) 0.0281, (◇) 0.553, (+) 5.212, and (∗) 20.7 mM oxalate. In the inset, the proton relaxivity rates at 0.1 MHz as a function of oxalate concentration are reported.

The experimental curves at 303 and 283 K are well reproduced, and the parameters reported in Table 1 are reasonable with respect to those found for similar Mn^{2+}-containing systems (*39*, *45*).

The overall message is that the profiles of nuclear relaxation enhancement can detect the water molecules coordinated to a manganese ion and can monitor changes in their coordination to the metal ion.

Interaction with Oxalate. Addition of increasing amounts of sodium oxalate does not produce any change in the relaxivity profiles (Figure 2). This indicates that oxalate does not displace any of the two water molecules bound to the Mn^{2+} ion in MnP and probably does not bind the metal ion at all. It had been already shown, through high-resolution

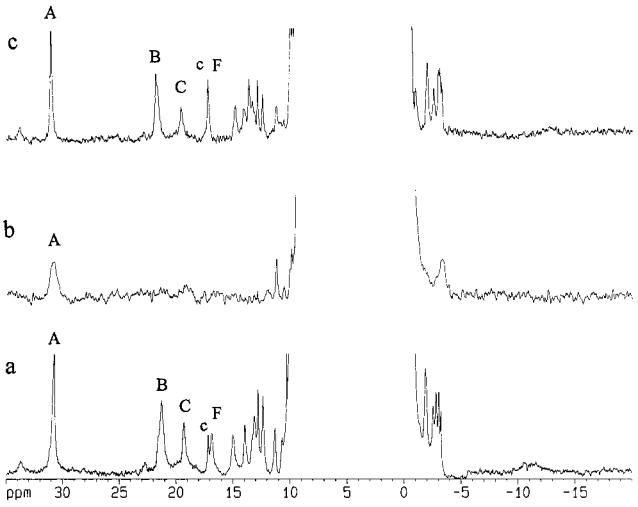

FIGURE 3: ^{1}H NMR spectra of MnP−CN$^-$ (a), of the MnPCN$^-$−$Gd_{1.0}^{3+}$ adduct (b), and of the MnP−$Gd_{1.0}^{3+}$ adduct in 50 mM oxalate (c). The spectra were recorded at 500 MHz, 298 K, in 25 mM Hepes buffer at pH 5.8. The labeling indicates corresponding signals in the spectra. Signal A is due to 3-CH_3, signal B to 8-CH_3, signal C and F respectively to the Hβ and Hβ' of the proximal histidine, and signal c to the Hδ_1 of the distal histidine.

^{1}H NMR experiments, that oxalate does not remove the Mn^{2+} from MnP (*26*), which can only be removed with EDTA (*26*).

The Binding of Lanthanides. During the catalytic cycle, Mn^{2+} is oxidized by the enzyme to Mn^{3+}. However, Mn^{3+} is not stable in solution and when complexed to the protein for times long enough to perform the characterization through NMRD measurements.

Preformed binding sites can host a variety of metal ions and they can do it better depending on whether their charge and the ionic radius are closer to those of the native ion. Trivalent lanthanide ions (Ln^{3+}) can be profitably used as probes of Mn^{3+} due to the similar ionic radii (*48*) and to the same charge. Ln^{3+} ions seem to be good probes also because they are hard ions and have high affinity for oxygen donor ligands, as Mn(III) does. Furthermore they are good probes for nuclear magnetic resonance, either as relaxation reagents or as shift reagents. As Gd^{3+} is a good relaxing reagent and Ce^{3+} is a good shift reagent, we have chosen these ions to characterize the interaction of MnP with trivalent metal ions, through relaxation measurements (Gd^{3+}) and high-resolution NMR studies (Ce^{3+}).

The interaction of Gd^{3+} with the cyanide adduct of MnP has been followed by high-resolution ^{1}H NMR, similar to the experiments performed to locate the binding site of Mn^{2+} (*26*). The ^{1}H NMR spectra of MnP−CN$^-$ without (a) and with about 1 equiv of Gd^{3+} (b) are shown in Figure 3. The signal due to 3-CH_3 experiences a broadening of 300 Hz, while the signals of 8-CH_3 and of β-CH_2 of the proximal His broaden at such an extent that they are not detectable anymore. The two species (Gd^{3+}-free and Gd^{3+}-bound) are in slow exchange one with the other, as evidenced by the simultaneous presence of the broad and sharp signals. The broadening of the heme resonances is caused by the dipolar coupling of their nuclear spins with the unpaired electron spins of Gd^{3+} ($S = {}^7/_2$). This contribution to the line width (which is equal to $(\pi T_{2M})^{-1}$) can be analyzed with the following equation, which takes into account the dipolar

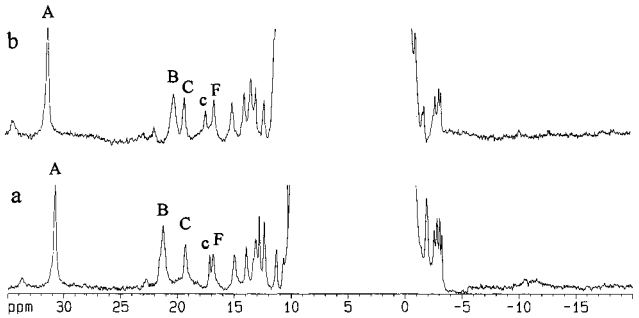

FIGURE 4: ^{1}H NMR spectra of MnP−CN$^-$ (a) and of the MnPCN$^-$−$Ce_{1.0}^{3+}$ adduct (b). The spectra were recorded at 600 MHz, 298 K, in 25 mM Hepes buffer at pH 5.8. The labeling of the signals is the same as that of Figure 3.

coupling of the nuclear spin with the electron spin (first term) (*42*) and with the static magnetic moment (Curie contribution, second term) (*49, 50*):

$$T_{2M}^{-1} = \frac{1}{15}\left[\frac{\mu_0}{4\pi}\right]^2 \frac{\gamma_n^2 g^2 \mu_B^2 S(S+1)}{r^6} \times \left[\frac{13\tau_c}{1+\omega_S^2\tau_c^2} + \frac{3\tau_c}{1+\omega_I^2\tau_c^2} + 4\tau_c\right] + \frac{1}{5}\left[\frac{\mu_0}{4\pi}\right]^2 \frac{g^4\mu_B^4\omega_I^2 S^2(S+1)^2}{(3kT)^2 r^6}\left[4\tau_r + \frac{3\tau_r}{1+\omega_I^2\tau_r^2}\right] \quad (5)$$

where all the symbols have already been defined.

At 500 MHz, the electron relaxation time of Gd^{3+} is longer than τ_r (*39*), and therefore τ_c is dominated by τ_r, which is calculated to be around 1.52×10^{-8} s, at 298 K, from the Stokes−Einstein equation. Applying eq *5*, the distance between the Gd^{3+} ion and the protons of 3-CH_3 is calculated to be around 16 Å. We have also estimated an upper limit of 10 Å for the distance between Gd^{3+} and the protons of 8-CH_3.

These data are similar to those found with Mn^{2+} and indicate that the binding site of Gd^{3+} is the same as that of the Mn^{2+}.

When Ce^{3+} is added to the CN$^-$ adduct of MnP, good high-resolution NMR spectra are still obtained (Figure 4). There is only a small broadening, as expected for the short relaxation times of Ce^{3+}, but the spectra experience sizable changes in the shifts of the signals. Indeed, Ce^{3+} has a high magnetic anisotropy and therefore gives rise to relatively large pseudocontact shifts (*51, 52*).

The intensity of signals of the MnPCN$^-$−Ce^{3+} adduct increases during the titration whereas the signals of the Mn-depleted MnP decrease. The MnPCN$^-$−Ce^{3+} species is in slow exchange with the Ce^{3+}-free species, consistent with the data on the Gd^{3+} adduct. The increase in intensity of the 3CH_3 NMR signal in the MnPCN$^-$−Ce^{3+} adduct with increasing amounts of Ce^{3+} is reported in Figure 5a. It can be observed that the binding is essentially stoichiometric, which sets the affinity constant to values larger than 10^5 M^{-1}.

All the protons of the heme substituents, even if to a different extent, experience a change in the shift values, as shown in the spectra of Figure 4. These data indicate that Ce^{3+} binds to the protein close to the heme moiety. From the comparison of the spectra with and without Ce^{3+}, a

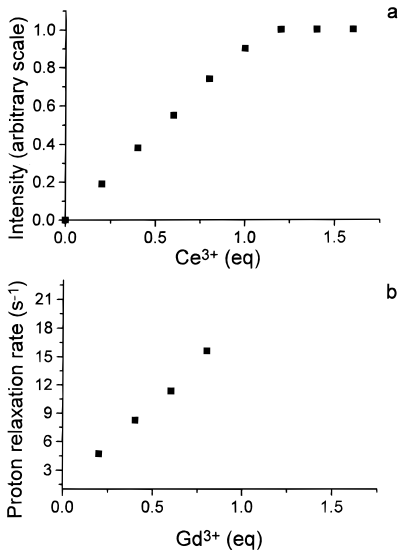

FIGURE 5: (a) Intensity (arbitrary scale) of the ^{1}H NMR signal of 3-CH_3 of MnP−CN^- with the addition of different amounts of Ce^{3+}, (b) experimental proton relaxation rates at 0.1 MHz, 303 K, pH 5.8, in 25 mM Hepes of a solution of 0.289 mM MnP−CN^- with addition of different amounts of Gd^{3+}.

tentative assignment can be performed. It is found that 8-CH_3 experiences a larger change in shift (−1 ppm) than 3-CH_3 (0.6 ppm). In the absence of the magnetic susceptibility parameters, a quantitative analysis cannot be performed; the data are, however, consistent with Ce^{3+} binding at the same site as Mn^{2+} and Gd^{3+}.

Relaxivity of MnPCN$^-$*−Gd*$^{3+}$. The uptake of Gd^{3+} has been monitored through NMRD measurements. Figure 5b shows the dependence of the experimental proton relaxation rates (taken at 0.1 MHz) of MnP−CN^- with increasing amounts of Gd^{3+} at pH 5.8 and 303 K. The last point of the titration corresponds to the maximum quantity of Gd^{3+} (1 equiv for a protein concentration of 0.20 mM) for which the protein is stable. The linear dependence, with the Gd^{3+} concentration, of the relaxivity and of the increase of line width in the high-resolution NMR spectra suggest an almost stoichiometric binding of Gd^{3+} to MnP−CN^-, indicating an affinity constant larger than 10^4−10^5 M^{-1}, as found for Mn^{2+} binding.

Two NMRD profiles, at two different temperatures, of the MnP−$Gd_{0.8}^{3+}$ adduct, normalized to a 1 mM metal concentration, are shown in Figure 6. These profiles are typical of a Gd^{3+}-protein adduct. As it appears from eq 1, the number of water molecules and their distance from the metal cannot be estimated independently from the NMRD profiles. Gd^{3+} has in general a larger coordination number than Mn^{2+}. This could be reached by a bidentate behavior of the carboxylate groups and/or by increasing the number of coordinated water molecules. By assuming three coordinating water molecules and following the same approach as for the MnPCN$^-$−Mn^{2+}, a fitting of the experimental NMRD profiles at 303 and 283 K is obtained with the parameters reported in Table 2.

Addition of oxalate to the MnP−$Gd_{0.8}^{3+}$ adduct causes a decrease in the relaxivity until it eventually reaches 0. Figure 7 shows the NMRD profiles of the MnP−$Gd_{0.8}^{3+}$ adduct, normalized to a 1 mM metal concentration, as a function of increasing amounts of oxalate. The inset plots the variation of relaxivity at 0.1 MHz versus the concentration of oxalate.

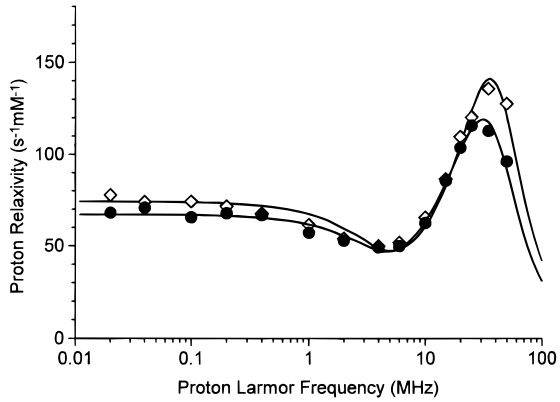

FIGURE 6: Proton relaxivity profiles of MnPCN$^-$−$Gd_{0.8}^{3+}$, normalized for a 1 mM metal concentration, in 25 mM Hepes buffer, pH 5.8, at 303 (◇) and 283 (●) K. The lines represent the best fit curves with the parameters reported in the Table 2.

Table 2: Best Fitting Parameters of the ^{1}H NMRD Profiles of the MnPCN$^-$−Gd^{3+} Systems

temperature (K)	303	283
τ_r (s)	1.34×10^{-8}	2.35×10^{-8}
τ_V (s)	1.6×10^{-11}	2.0×10^{-11}
Δ (cm^{-1})	2.5×10^{-2}	2.3×10^{-2}
D^a (cm^{-1})	2.6×10^{-2}	2.6×10^{-2}
τ_m (s)	1.9×10^{-7}	3.1×10^{-7}
r (Å)	3.00	3.00

[a] D is the static ZFS parameter.

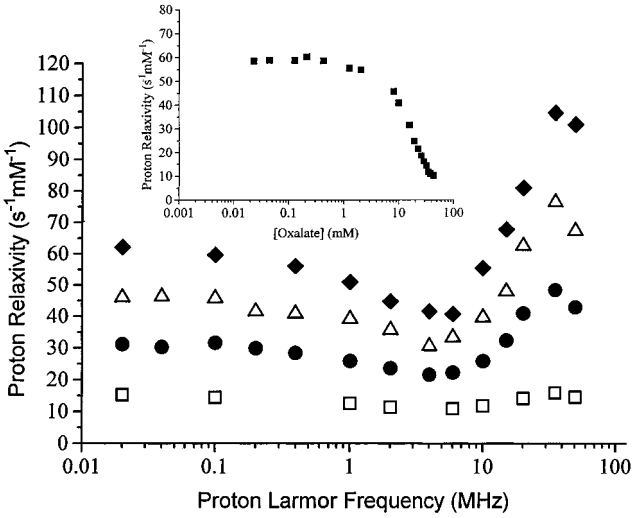

FIGURE 7: Proton relaxivity profiles of MnPCN$^-$−$Gd_{0.8}^{3+}$, normalized for a 1 mM protein concentration, at 303 K, in 25 mM Hepes, pH 5.8, at different concentrations of oxalate: (◆) without oxalate and with (△) 8, (●) 16, and (□) 32 mM oxalate. In the inset, the proton relaxivity rates as a function of oxalate concentration at 0.1 MHz are reported.

The effect starts to be present for oxalate concentrations around 4 mM and is essentially completed for concentrations around 60 mM. These data indicate that addition of oxalate perturbs the coordination of Gd^{3+} in MnP−CN^-, either by displacing the coordinated water molecules or by removing Gd^{3+} from the protein.

To discriminate between these two possibilities, we have recorded high-resolution ^{1}H NMR spectra on the last sample of the titration with oxalate. The spectrum is essentially the same as that of MnP−CN^- before addition of Gd^{3+} (Figure 3c); namely, the heme resonances have their normal line

widths. Therefore, oxalate displaces Gd^{3+} from coordination to the protein.

By adding oxalate to the MnP−$Ce_{1.0}^{3+}$ adduct (present at ∼1 mM concentration) to a concentration of 20 mM in oxalate, the intensity of the signals of the spectrum of Figure 4b reduces to less than half and the signals present in the spectrum of Figure 4a are obtained again (with an intensity ratio of 3:7 MnP−Ce^{3+} complex/MnP−Ce^{3+} free). By increasing the oxalate concentration to 70 mM, the spectrum of Figure 4b disappears completely and the spectrum of Figure 4a is obtained again. It can be therefore concluded that oxalate also removes Ce^{3+} from its coordination site. This behavior is totally consistent with what is observed with the Gd^{3+} adduct. It should be noted that the amount of oxalate required to remove the metal ion is relatively large at the present protein concentrations.

The physiological concentrations of oxalate produced in *P. chrysosporium* cultures have been reported to range from 0.1 to 2 mM (*35*, *53*). The oxalate concentrations required to remove Gd^{3+} and Ce^{3+} from the protein are slightly larger than the physiological ones even if they are of similar order of magnitude.

CONCLUSIONS

This research shows that oxalate does not remove water from the coordination sphere of Mn^{2+} bound to MnP and that it does not remove Mn^{2+} from the coordination site in the protein. We have then used Gd^{3+} and Ce^{3+} as probes for Mn^{3+}. Gd^{3+} binds with high affinity at the site of Mn^{2+} as shown by the broadening of the heme signals in a way similar to that observed for Mn^{2+}. For Ce^{3+}, pseudocontact shifts are qualitatively consistent with binding at the same site. In these adducts the presence of oxalate, at millimolar concentrations as used in this study and in the kinetic measurements (*33*−*35*), for which the ratio between protein and oxalate concentrations mimics physiological conditions, leads to the formation of Ln−oxalate complexes which do not interact with the protein. This has been shown by the reappearance of the NMR signals experienced by the manganese-depleted MnP−CN^- and by the disappearance of the NMRD enhancement which was induced by the bound Gd^{3+}. However, there is no evidence of formation of ternary protein−Ln−oxalate complexes, as the disappearance of shift variation or line broadening follows the same pattern as the decrease in relaxivity.

These experimental data support the idea that both Mn^{2+} and Mn^{3+} bind to MnP and that oxalate does not interact with Mn^{2+} but binds Mn^{3+} in such a way that then the Mn^{3+}−oxalate complex diffuses away. This is indeed consistent with the observation that Mn^{3+} forms, in general, stronger complexes than Mn^{2+} (*54*, *55*) with bidentate carboxylate ligands. However, the available kinetic experiments (*33*, *34*) and our present data do not allow us to distinguish between whether a transient ternary complex (MnP−Mn^{3+}−oxalate) forms before diffusion of the Mn−oxalate complex off of the active site and whether the Mn^{3+} diffuses away from the active site prior to complexation by oxalate.

This scheme is not consistent with a previously proposed mechanism derived from kinetic experiments on compound II reported by some of us (*34*). It is, however, consistent with conclusions reached by others (*33*) proposing that free Mn^{2+} is the substrate for compound II. Our stopped flow experiments showed that the reduction of compound II to the resting state by Mn^{2+} required oxalate. Maximal rates were observed at concentrations of oxalate which favored a 1:1 ratio of oxalate/Mn^{2+}. At higher oxalate concentrations, where the 2:1 oxalate/Mn^{2+} complex is favored, no reaction was observed. It was therefore concluded that it is the 1:1 oxalate/Mn^{2+} complex which reacts with compound II, which is in conflict with the results of the present study showing that such a complex does not exist.

There is a mechanism that is consistent with both the kinetic and spectroscopic data which is shown below.

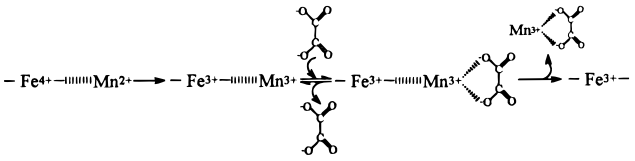

This mechanism shows that oxalate does not bind Mn^{2+} and that the oxidation of Mn^{2+} by compound II produces the resting state enzyme and Mn^{3+}, prior to complexation of Mn^{3+} by oxalate. Addition of oxalate would drive the reaction even more toward the products, yielding the results we observed in the stopped flow experiments. This mechanism would explain both the kinetic results and the spectroscopic results of the present paper.

An alternate explanation could consider that the present study characterized the binding of Mn/oxalate to the ferric enzyme, not to compound II. It might occur that in the case of compound II a ternary complex with Mn^{2+} and oxalate is formed while it is not formed in the case of the resting enzyme. This would be consistent with the larger positive charge of compound II relative to resting ferric enzyme. This in turn would weaken the donor capacity of propionate 6 and then would favor chelation by oxalate. However, even though this different behavior cannot be ruled out, the similar affinity of Mn^{2+} for the native protein and for the cyanide adduct seems to indicate that this is not the case. This mechanism, in addition to the one described above, is presently being tested by both kinetic and spectroscopic methods.

ACKNOWLEDGMENT

Professor Claudio Luchinat is warmly acknowledged for the helpful discussion on the analysis of the NMRD profiles. This research has been partially financed by the Progetto Strategico "Tecnologie Chimiche Innovative", 95.04535.ST74, by Comitato "Scienze e Tecnologie Ambiente e Habitat", 93.001179.CT13, Consiglio Nazionale delle Ricerche (CNR), by the European Community (Program Human Capitol and Mobility), CH RX CT 940540, by the United States Department of Energy Grant DE-FG02-87ER13690 to M.T., and by the European Community, FAIR-CT95-0805 program.

REFERENCES

1. Wariishi, H., Valli, K., and Gold, M. H. (1991) *Biochem. Biophys. Res. Commun. 176*, 269−275.
2. Huynh, V. B., and Crawford, R. L. (1985) *FEMS Microbiol. Lett. 28*, 119−123.
3. Glenn, J. K., and Gold, M. H. (1985) *Arch. Biochem. Biophys. 242*, 329−341.

4. Orth, A. B., Royse, D. J., and Tien, M. (1993) *Appl. Environ. Microbiol. 59*, 4017−4023.
5. Glenn, J. K., Akileswaran, L., and Gold, M. H. (1986) *Arch. Biochem. Biophys. 251*, 688−696.
6. Sundaramoorthy, M., Kishi, K., Gold, M. H., and Poulos, T. L. (1994) *J. Biol. Chem. 269*, 32759−32767.
7. Welinder, K. G., and Gajhede, M. (1993) in *Plant Peroxidases Biochemistry and Physiology* (Greppin, H., Rasmussen, S. K., Welinder, K. G., and Penel, C., Eds.) pp 35−42, University of Copenhagen and University of Geneva, Geneva, Switzerland.
8. Poulos, T. L., Freer, S. T., Alden, R. A., Edward, S. L., Skogland, U., Takio, K., Eriksson, B., Xuong, N., Yonetani, T., and Kraut, J. (1980) *J. Biol. Chem. 255*, 575−580.
9. Erman, J. E., Vitello, L. B., Miller, M. A., and Kraut, J. (1992) *J. Am. Chem. Soc. 114*, 6592−6593.
10. Vitello, L. B., Erman, J. E., Miller, M. A., Wang, J., and Kraut, J. (1993) *Biochemistry 32*, 9807−9818.
11. Erman, J. E., Vitello, L. B., Miller, M. A., Shaw, A., Broen, K. A., and Kraut, J. (1993) *Biochemistry 32*, 9798−9806.
12. Wariishi, H., Akileswaran, L., and Gold, M. H. (1988) *Biochemistry 27*, 5365−5370.
13. Banci, L. (1997) *J. Biotechnol. 53*, 253−263.
14. Everse, J., and Everse, K. E. (1991) in *Peroxidases in chemistry and biology*, Vols. 1 and 2, CRC Press, Boca Raton, FL.
15. Mino, Y., Wariishi, H., Blackburn, N. J., Loehr, T. M., and Gold, M. H. (1988) *J. Biol. Chem. 263*, 7029−7036.
16. Blumberg, W. E., Peisach, J., Wittenberg, B. A., and Wittenberg, J. B. (1968) *J. Biol. Chem. 243*, 1854.
17. Kishi, K., Kusters-van Someren, M., Mayfield, M. B., Sun, J., Loehr, T. M., and Gold, M. H. (1996) *Biochemistry 35*, 8986−8994.
18. Banci, L., Bertini, I., Kuan, I., Tien, M., Turano, P., and Vila, A. J. (1993) *Biochemistry 32*, 13483−13489.
19. Banci, L., Bertini, I., Pease, E. A., Tien, M., and Turano, P. (1992) *Biochemistry 31*, 10009−10017.
20. de Ropp, J. S., La Mar, G. N., Wariishi, H., and Gold, M. H. (1991) *J. Biol. Chem. 266*, 15001−15008.
21. Satterlee, J. D., and Erman, J. E. (1991) *Biochemistry 30*, 4398−4405.
22. Satterlee, J. D., Russell, D. J., and Erman, J. E. (1991) *Biochemistry 30*, 9072−9077.
23. Banci, L., Bertini, I., Turano, P., Ferrer, J. C., and Mauk, A. G. (1991) *Inorg. Chem. 30*, 4510−4516.
24. Chen, Z. G., de Ropp, J. S., Hernandez, G., and La Mar, G. N. (1994) *J. Am. Chem. Soc. 116*, 8772−8783.
25. Veitch, N. C., Gao, Y., and Welinder, K. G. (1996) *Biochemistry 35*, 14370−14380.
26. Banci, L., Bertini, I., Bini, T., Tien, M., and Turano, P. (1993) *Biochemistry 32*, 5825−5831.
27. Whitwam, R. E., Brown, K. R., Musick, M., Natan, M. J., and Tien, M. (1997) *Biochemistry 36*, 9766−9773.
28. Sakurada, J., Takahashi, S., and Hosoya, T. (1986) *J. Biol. Chem. 261*, 9657−9662.
29. Veitch, N. C., and Williams, R. J. P. (1991) in *Biochemical and Physiological Aspects of Plant Peroxidases* (Lobarzewski, J., Greppin, H. L., Penel, C., and Gaspar, T. H., Eds.) University of Geneva, Geneva, pp 99−109.
30. La Mar, G. N., Hernàndez, G., and de Ropp, J. S. (1992) *Biochemistry 31*, 9158−9168.
31. Turano, P., Ferrer, J. C., Cheesman, M. R., Thomson, A. J., Banci, L., Bertini, I., and Mauk, A. G. (1995) *Biochemistry 34*, 13895−13905.
32. Wariishi, H., Dunford, H. B., MacDonald, I. D., and Gold, M. H. (1989) *J. Biol. Chem. 264*, 3335−3340.
33. Wariishi, H., Valli, K., and Gold, M. H. (1992) *J. Biol. Chem. 267*, 23688−23695.
34. Kuan, I.-C., Johnson, K. A., and Tien, M. (1993) *J. Biol. Chem. 268*, 20064−20070.
35. Kuan, I.-C., and Tien, M. (1993) *Proc. Natl. Acad. Sci. U.S.A. 90*, 1242−1246.
36. Whitwam, R. E., Gazarian, I. G., and Tien, M. (1995) *Biochem. Biophys. Res. Commun. 216*, 1013−1017.
37. Paszczynski, A., Huynh, V. B., and Crawford, R. (1985) *FEMS Microbiol. Lett. 29*, 37−41.
38. Koenig, S. H., and Brown, R. D., III (1987) in *NMR Spectroscopy of Cells and Organisms* (Gupta, R. K., Ed.) Vol. II, pp 75, CRC Press, Boca Raton, FL.
39. Banci, L., Bertini, I., and Luchinat, C. (1991) *Nuclear and electron relaxation, The magnetic nucleus-unpaired electron coupling in solution*, VCH, Weinheim, Germany.
40. Luchinat, C., and Xia, Z. (1992) *Coord. Chem. Rev. 120*, 281−307.
41. Kennedy, S. D., and Bryant, R. G. (1985) *Magn. Reson. Med. 2*, 14−19.
42. Solomon, I. (1955) *Phys. Rev. 99*, 559−565.
43. Bloembergen, N., and Morgan, L. O. (1961) *J. Chem. Phys. 34*, 842−850.
44. Banci, L., Bertini, I., Briganti, F., and Luchinat, C. (1986) *J. Magn. Reson. 66*, 58−65.
45. Bertini, I., Luchinat, C., Mincione, G., Parigi, G., Gassner, G. T., and Ballou, D. P. (1996) *JBIC, J. Biol. Inorg. Chem. 1*, 468−475.
46. Stokes, G. (1956) *Trans. Cambridge Philos. Soc. 9*, 5.
47. Einstein, A. (1956) *Investigations on the Theory of the Brownian Movement*, Dover, Publications, New York.
48. Weast, R. C. (1986) *Handbook of Chemistry and Physics*, CRC Press, Boca Raton, FL.
49. Vega, A. J., and Fiat, D. (1976) *Mol. Phys. 31*, 347−362.
50. Gueron, M. (1975) *J. Magn. Reson. 19*, 58−66.
51. Bertini, I., and Luchinat, C. (1996) *Coord. Chem. Rev. 150*.
52. Peters, A. R., Huskens, J., and Raber, D. J. (1996) *Prog. NMR Spectrosc. 28*, 283−350.
53. Kishi, K., Wariishi, H., Marquez, L., Dunford, H. B., and Gold, M. H. (1994) *Biochemistry 33*, 8694−8701.
54. Martell, A. E., Sillen, L. G., Schwarzenbach, G., and Bierrum, J. (1964) *Stability constants of metal-ion complexes*, The Chemical Society, London, England.
55. Martell, A. E., and Hancock, R. D. (1996) *Metal complexes in aqueous solutions*, Plenum Press, New York and London, England.

BI972879+